

On the internal morphologies of high-modulus polyethylene and polypropylene fibres

M. I. ABO EL-MAATY*, R. H. OLLEY†, D. C. BASSETT
J. J. Thomson Physical Laboratory, Whiteknights, Reading RG6 6AF, UK
E-mail: r.h.olley@reading.ac.uk

High modulus polyethylene fibres, both melt and gel-spun, contain the same longitudinal density deficient regions, revealed by permanganic etching, as were found in specimens of the same fibres after treatment by the Leeds high temperature compaction process. For these materials a new model of fibre structure is proposed, which develops as a consequence of nucleation on an extended network of entangled molecules permeating the fibres. Subsequent growth into spaces between the network will encounter stresses due to the contraction on crystallization leading to distributed density deficient regions of high free volume. Each of the four commercial PE fibres examined differs from the others in its characteristic outline and the details of its internal substructure. The structure of commercial polypropylene fibres is also compared. © 1999 Kluwer Academic Publishers

1. Introduction

During the morphological examination at Reading, of the products obtained at the University of Leeds by hot compaction of high-modulus polyethylene [1–4] and polypropylene [5] fibres, it became evident that the fibres themselves contained a structure of internal defects. These were first seen in compacted melt-spun polyethylene fibres [1, 2] both in the form of craters in etched cross-sections, and sometimes as recrystallized regions several microns long running parallel to the fibre axis after etching of longitudinal sections. It was suggested [2] that these defects are density-deficient regions, i.e. of excess free volume, which were formed in the fibres during their production, as a consequence of a fixed mass of material, crystallizing within, and nucleating on, a rather rigid internal confining framework. At high treatment temperatures the excess free volume could be concentrated by melting and recrystallizing into a linear hole at the centre of the recrystallized defective region [4]. Moreover, defects were seen in fibres compacted several degrees below the optimum temperature for the process [3], before melting has occurred to any large extent, and it is around these defects that internal melting of the fibres starts [4]. Similar defects were also seen in compactations of gel-spun and melt-kneaded polyethylene (PE) fibres [5, 6]. To elucidate the nature of these defects, it was desired to study the individual fibres, without heat treatment or compaction, by similar means of etching and electron microscopy.

There is still much uncertainty concerning the structure of polymer fibres, and though many models were put forward in previous decades, there does not appear

to be a recent review. Fibres have been generally examined by indirect methods such as X-ray scattering, birefringence, etc., which reveal the chain axis orientation but fail to provide adequate information about the arrangement of molecules in real space or chain extension [7, 8]. It has however been common to consider that the structure is based on “microfibrils” or “nanofibrils”, and features claiming to fit this description, accompanied by small lamellar overgrowths, are seen even with modern techniques such as scanning force microscopy [9]. In practice the properties of fibres differ widely according to their method of production, degree of extension, molecular weight of polymer, etc. This has allowed some hypotheses to be put forward regarding the existence of a network of entangled long molecules and its effect on these properties. A recent penetrating analysis of this type [10] has suggested that “the strength of high modulus polyethylene fibres is determined by microscopic defect structures, which are distributed at such high frequency that no size effects [in relation to fibre diameter or length] arise from them”. Such structures would exist in addition to the “microfibrils” referred to above, and in this work direct morphological investigation using modern techniques for electron microscopy has revealed what these might be, and from this hitherto unknown common factors for fibres in general. For example in Spectra the microstructure thus revealed differs from previous best inferences based on models [12]. Even though these models were combined with evidence such as periodicities observed in electron diffraction [13], direct real space observations must change understanding of fibre structure and properties.

* *Present address:* Department of Physical Science, Faculty of Science, Mansoura University, Mansoura, Egypt.

† author to whom all correspondence should be addressed.

Detailed electron microscopy of polymers is especially difficult when they are in the form of fibres. The chlorosulphonation technique has been applied [11] but the technique has its limitations [14]. Even the use of fuming nitric acid degradation, which proved very productive for obtaining lamellar thicknesses in ultra-high modulus drawn bulk materials [15, 16], is limited in its application to fibres [17].

In the present work, five samples of high modulus fibres have been investigated, using the permanganic etching technique followed by scanning and transmission electron microscopy. The principal aim is to describe a suitable morphological, and if possible, molecular structural model for high modulus polymer fibres, which could be applied to further development of these materials.

2. Experimental

2.1. Materials

The four types of high modulus PE and the one type of polypropylene (PP) fibre and their properties are given in Table I. In the present work, the fibres have been examined only as-received, although in subsequent work the same techniques have been used for PE fibres after annealing treatments close to their respective melting points.

2.2. Specimen preparation

Transverse sections of the original fibres were obtained by embedding them between two sheets of polystyrene-(ethylene-propylene) block copolymer Kraton G1650 (Shell) and cutting with a diamond knife. For longitudinal sections, the fibres were embedded on the surface of a layer of Kraton G1650, and etched directly.

The transverse sections were examined under the SEM, while longitudinal sections were examined by replication and TEM.

Replicas for TEM were obtained using a two stage technique. A first replica was made by applying a sheet of cellulose acetate moistened with acetone on the etched surface. The acetate sheet was then coated with Ta/W at an angle of approx. 35° to the horizontal, followed by carbon vertically onto the replica. This shadowed carbon film was then retrieved on copper grids after solvent extraction.

TABLE I

Fibre name	Type	Manufacturer	M_w (kg/mol)	Measured average longitudinal defect length
Certran	Melt-spun PE	Hoechst Celanese	150	7 μm
Spectra	Gel-spun PE	Allied Signal	1500	30 μm
Dyneema	Gel-spun PE	DSM	1300	25 μm
Tekmilon	Melt-kneaded PE	Mitsui Petrochemical	700	20 μm
Leolene	Melt-spun PP	F. Drake & Co.	?	3 μm

2.3. Etching reagents

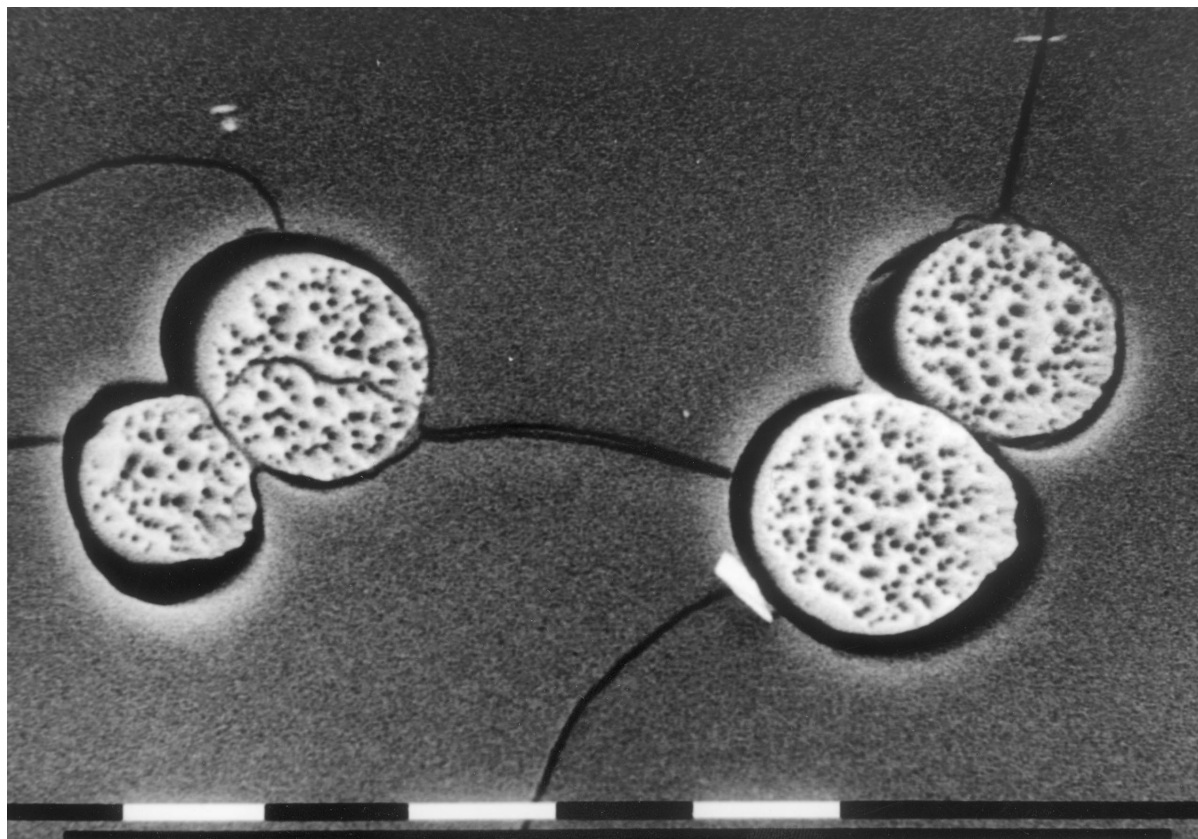
Two different etching reagents were employed in this work to enhance different views of the morphology. Their compositions were as follows:

- “Dry etchant”: 1% w/v potassium permanganate in a mixture of 2 vols. concentrated sulphuric acid to 1 vol. dry orthophosphoric acid (prepared by boiling off water to b.p. 260 °C). This, applied to transverse sections for 75 minutes, is referred to as a “dry etch”.
- “Wet etchant”: 1% w/v potassium permanganate in a mixture of 10 vols. concentrated sulphuric acid to 4 vols. orthophosphoric acid (Merck reagent, min. 85%) to 1 vol. distilled water. This, as applied to transverse sections for 45 minutes, is referred to as a “short wet etch”, and for 2 hours to longitudinal sections, as a “long wet etch”.

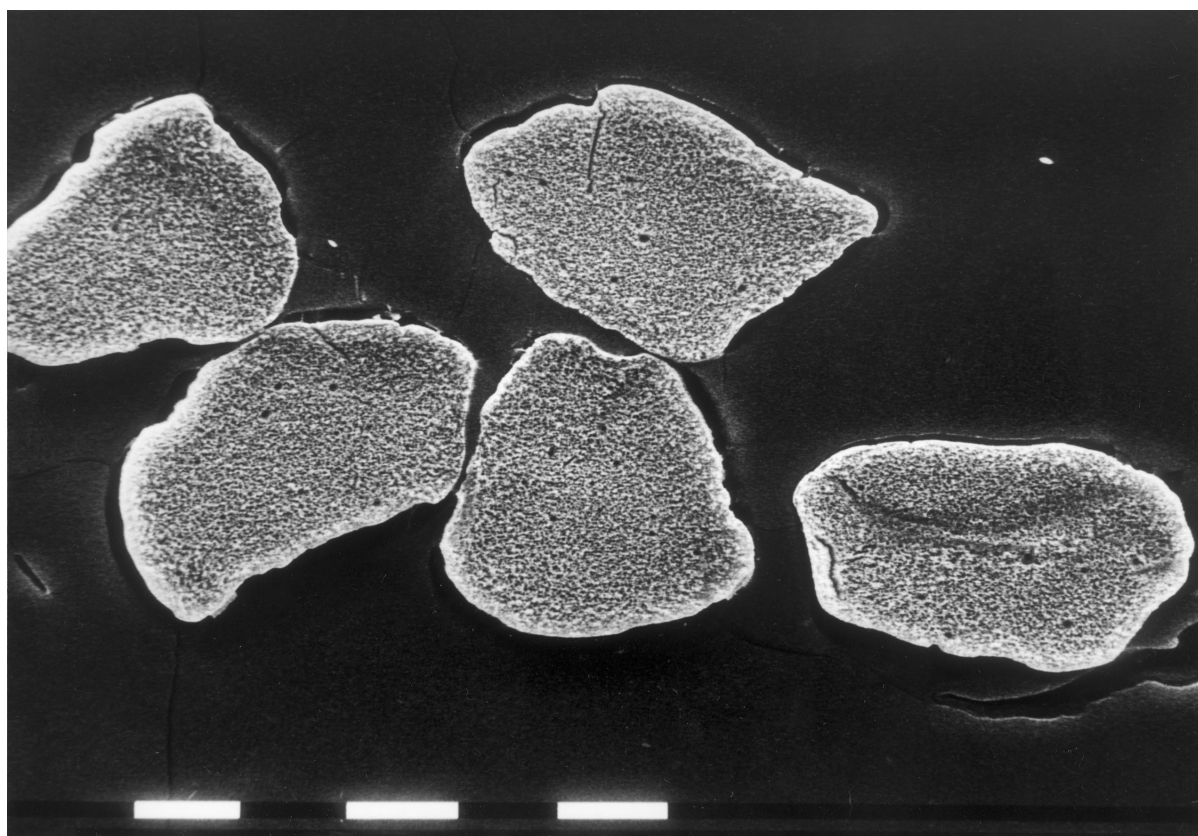
3. Results and discussion

3.1. Polyethylene

The first observation is the variety of cross-sectional shapes and internal textures observed for the fibres, which is most evident at low magnification, Fig. 1. Each type of fibre has its own characteristic appearance which presumably reflects the different conditions of formation. The circular sections of the Certran (formerly Tenfor) fibres (a) are familiar from earlier work, as is their variation in diameter. The fibres are prepared by the melt being spun through a circular spinneret, and subsequently drawn 40 times. The notable variation in diameter is liable to arise from different degrees of retraction after spinning, but for this particular system is unlikely to have a great effect on properties [18]. In contrast, the gel spun fibres have irregular sections which relate to the shrinkage of a circular thread of gel following solvent loss [12]. This is to be expected from gel-spun fibres in general [19] since with variations the fibres are spun from a semi-dilute solution from which the solvent is removed by evaporation or solvent extraction to give a porous structure (sometimes referred to as a “Xerogel”) which is then drawn to give the final product [20]. The irregular sections of the Spectra fibre (b) are also apparent in compactions [21] while the bean-like sections of the Dyneema fibres (c) suggest a more drastic process, suggesting the collapse of the fibre while constrained by a skin formed in an earlier stage. Tekmilon fibres (d) have essentially circular sections, which suggest only a slight degree of collapse from the circular cross section imposed by surface tension. This might be partially due to a higher concentration of polymer in the solution, as implied by the term “melt-kneaded”, in which the paraffin acts as a lubricant rather than a true solvent. If collapse does take place after a skin is formed, then the final shape will be determined by the time the skin is formed: if early, when there is still much solvent present, the final result will be a bean like shape as shown by the Dyneema fibres here. In the development of the Spectra process, in experiments where the original solvent (typically decalin)



(a)

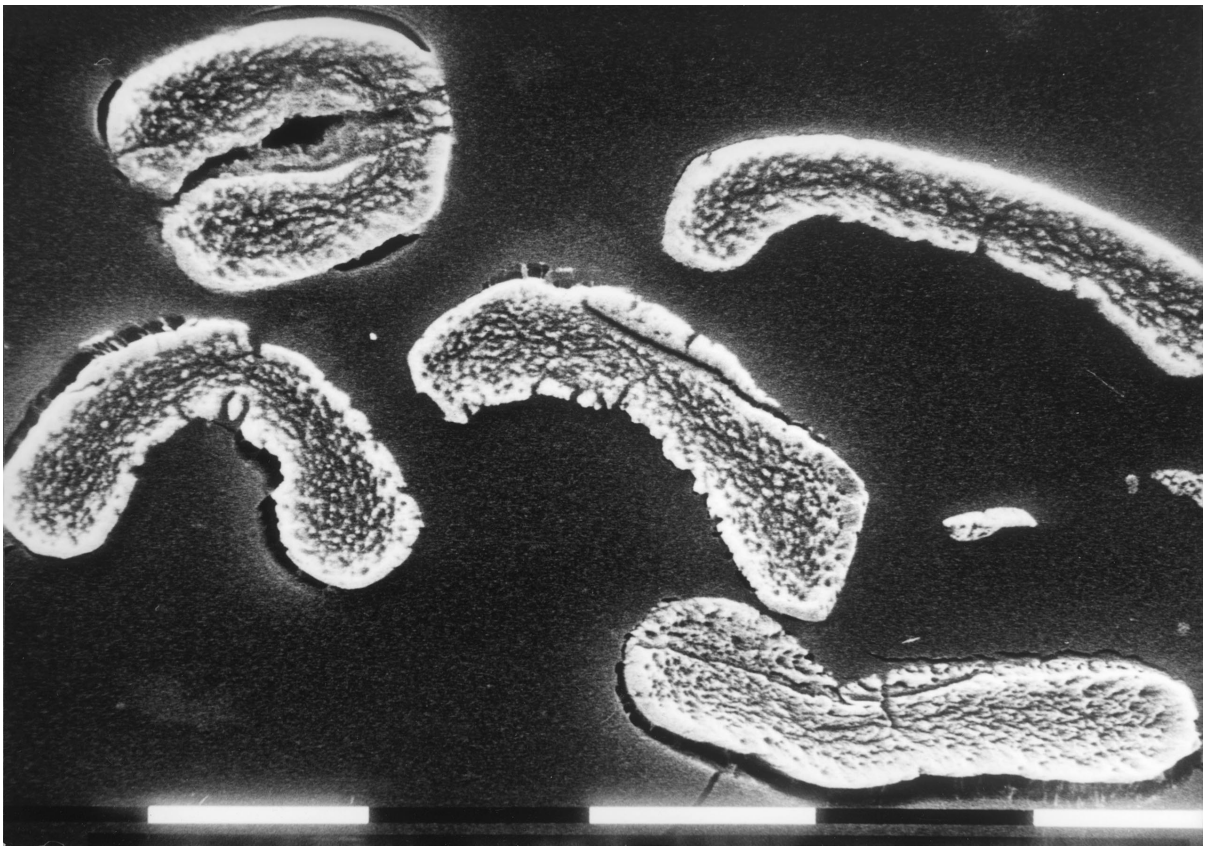


(b)

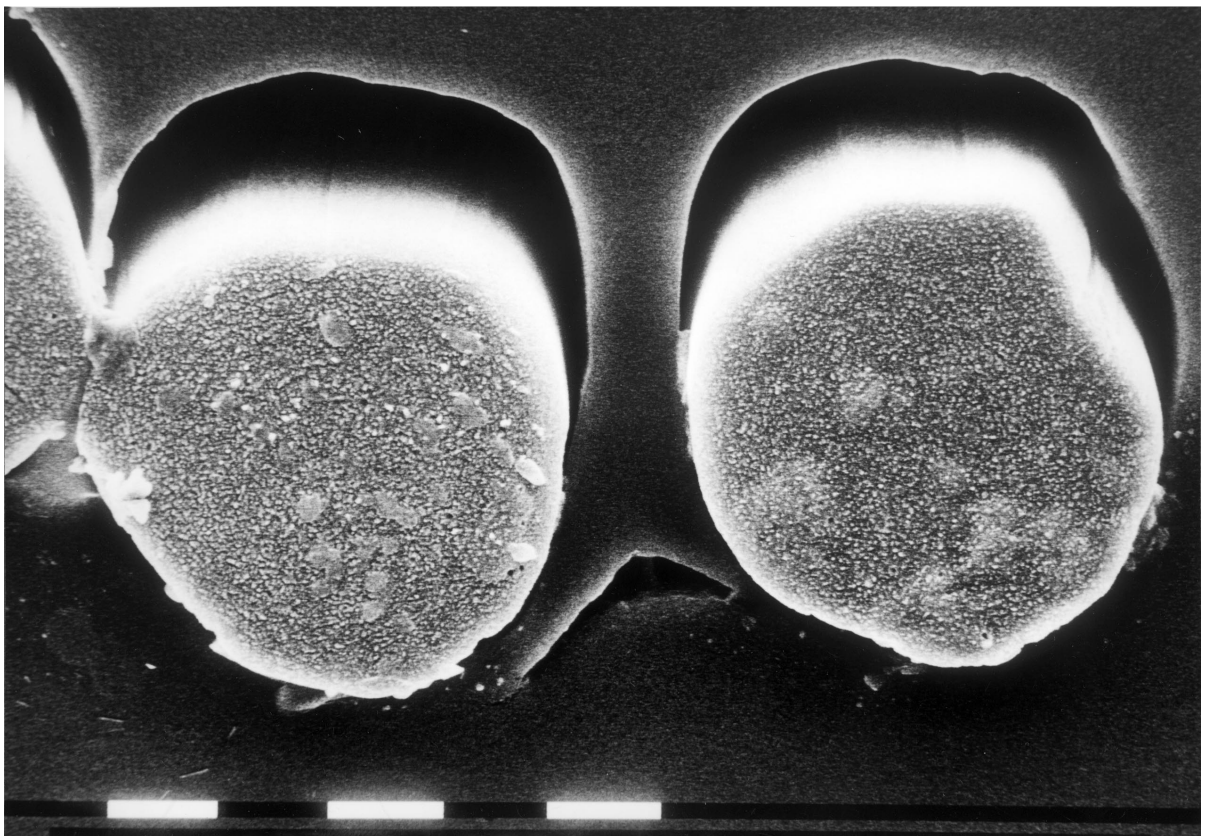
Figure 1 Morphology of fibre cross-sections etched with "short wet" etch: (a) Certran, (b) Spectra, (c) Dyneema and (d) Tekmilon. SEM of untilted specimens at lower magnification. All bars = 10 μm . (Continued)

was replaced by an extraction solvent, Prevorsek [12] observed a pattern where the section tends to change from circular to irregular as the solvent boiling point increased.

The fibrillar defects first revealed in the transverse sections by permanganic etching during the investigation of the compacted fibres [2, 21], are now confirmed to be present in the originals also, and not to be produced



(c)

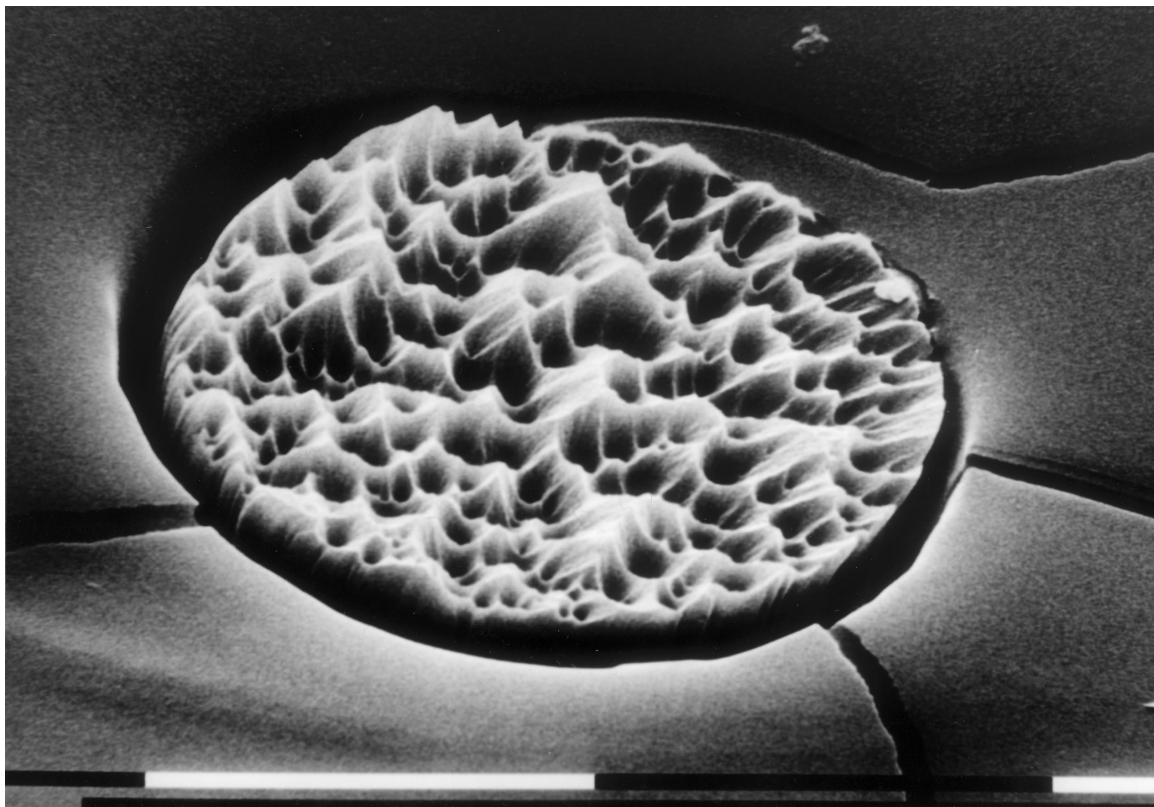


(d)

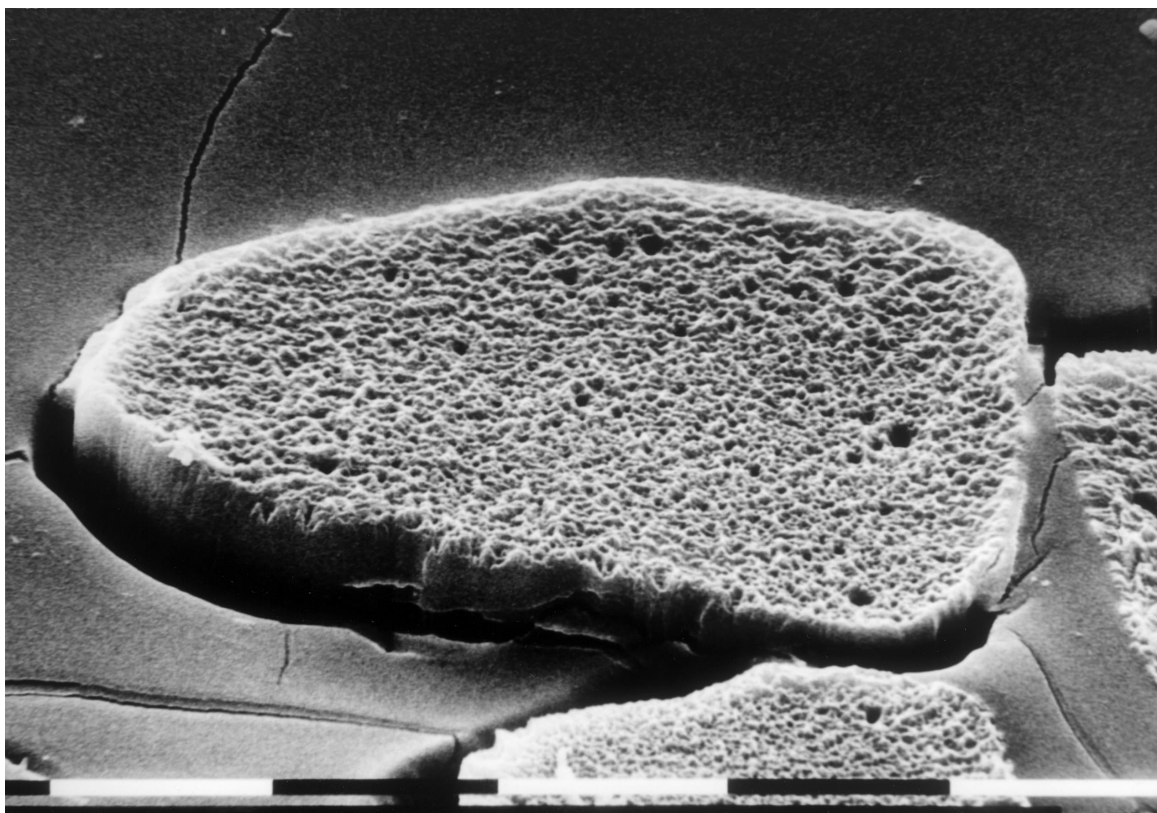
Figure 1 (Continued).

by the compaction process, though their presence was deduced from the necessity of there being free volume to initiate the observed melting processes [2]. They can be seen in Figs 1a and 2a, showing scanning electron

micrographs of etched transverse sections of the original Certran fibres. At the low magnification of Fig. 1 the defective regions are identified by dark spots, but at higher magnification Fig. 2 these are resolved as the



(a)

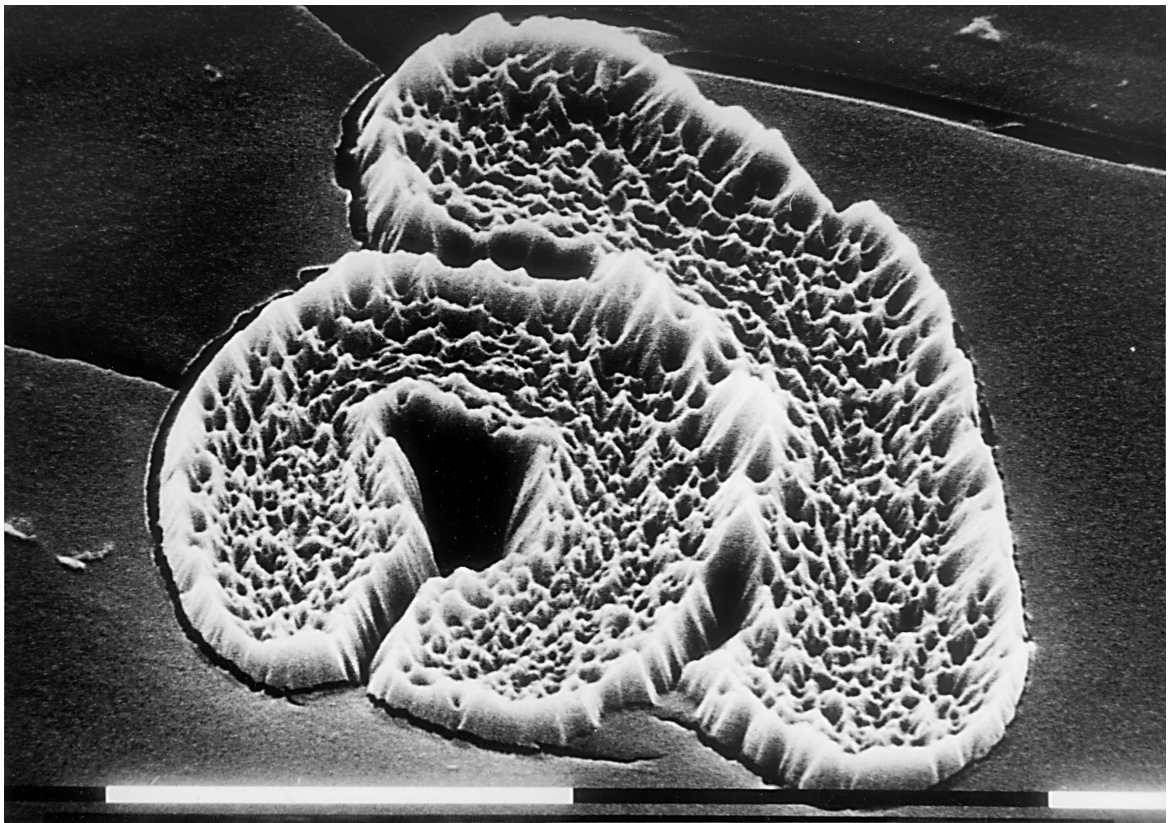


(b)

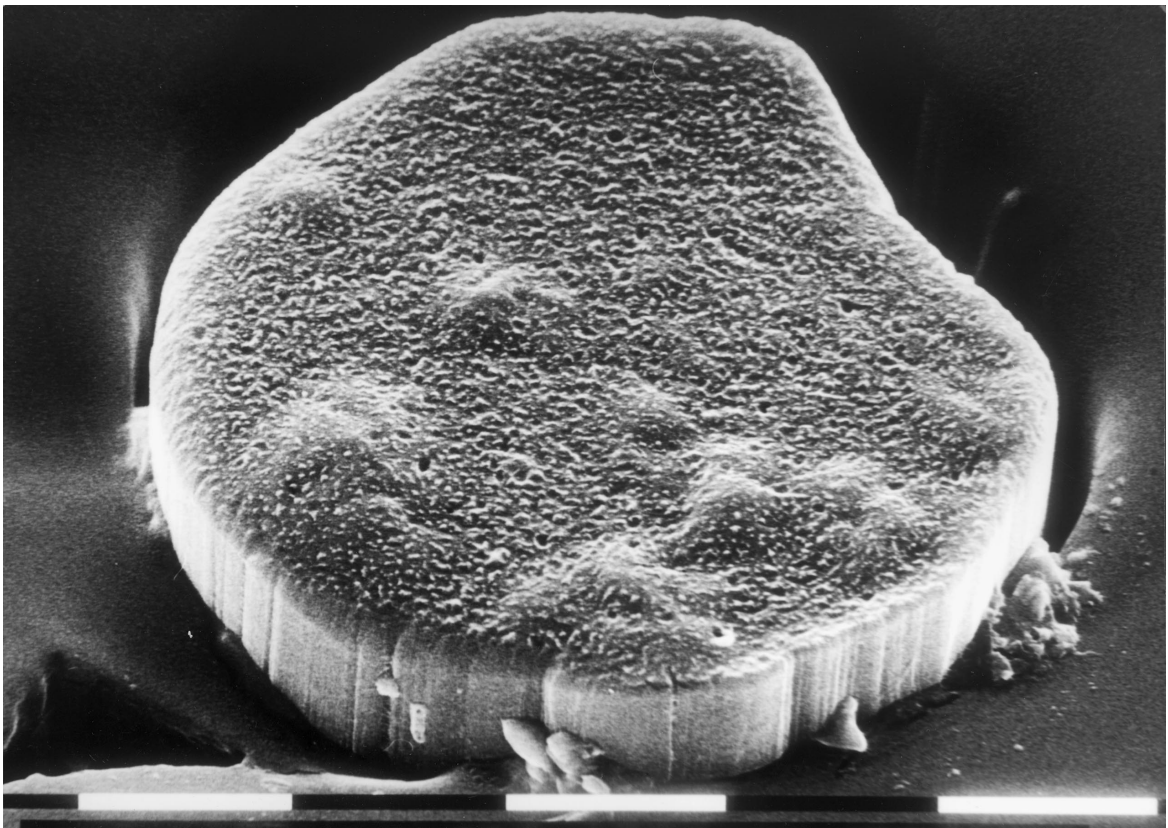
Figure 2 Morphology of fibre cross-sections etched with "short wet" etch: (a) Certran, (b) Spectra, (c) Dyneema and (d) Tekmilon. SEM of tilted specimens. All bars = 10 μm . (Continued)

centres of craters in the etched surface. The lower magnification pictures are similar in scale, and from these it is apparent that the craters are fewer in number in the melt-spun fibres Certran and PP than in those pro-

duced with a solvent, Spectra and Dyneema, or a lubricant, Tekmilon. Except in Dyneema, there is little evidence for skin-core variation (although there is some evidence that in Certran the craters become smaller near



(c)



(d)

Figure 2 (Continued).

the outside of the fibre, but this can only be seen in lower temperature compactions, where the outside is more protected from etching than in the individual fibres [3]). However, all materials show apparent local variations in density of cratering, which will be discussed below.

3.2. Generation of the crater structure

The actual defects themselves are very long (several μm) narrow density-deficient regions, which are penetrated preferentially by the etchant. In previous work [2] when these were examined by TEM using a replication technique, it was found that threads of the replicating

Mechanism for different etching rates on high modulus PE fibres

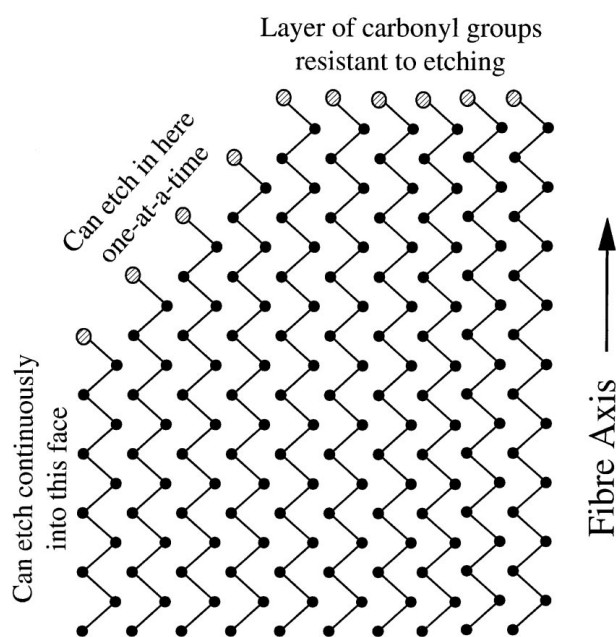


Figure 3 Schematic mechanism of etching of oriented polyethylene fibres.

material could emanate from these narrow cylindrical channels, presumably drawn out from material which had penetrated some way into them. The initial state of the defects has been developed over time by the etchant into a crater, indicative of a net rate of attack at an angle to the chain axis. This may arise as follows. Over the initial cut surface the etchant would be attempting to remove material by attacking down the chain-axis; etchant which has percolated down inside the defect would be attacking the chains from the side. This situation is represented by the schematic block of oriented PE shown in Fig. 3. The molecules in these fibres are oriented parallel to their neighbours in crystallographic array, preventing or at least hindering oxidative etchants from attacking down the fibre length. On the crystallographic side surfaces on the exterior of fibres and within the defects, one may speculate that the accessibility of the hydrogen atoms on the $-\text{CH}_2-$ groups allows oxidation so that the molecular stems be cut into fragments which split off, but on the top surface a phalanx of oxidized $-\text{COOH}$ groups is formed, which resists penetration. This is the same mechanism whereby the basal surface of lamellar crystals are resistant to continued attack by fuming nitric acid or permanganic etchants, once the interlamellar material has been digested [22]. However, at the corners it is possible to etch away individual units on successive stems to give the observed diagonal profile. Where narrow channels either exist or have been eaten out of the defective regions within the fibres, the etchant can penetrate these and attack diagonally, leading to a conical hole or crater into the end surface. The evidence for such a mechanism is the fact that, under these conditions, this diagonal angle appears more or less constant for different etchants. Conditions

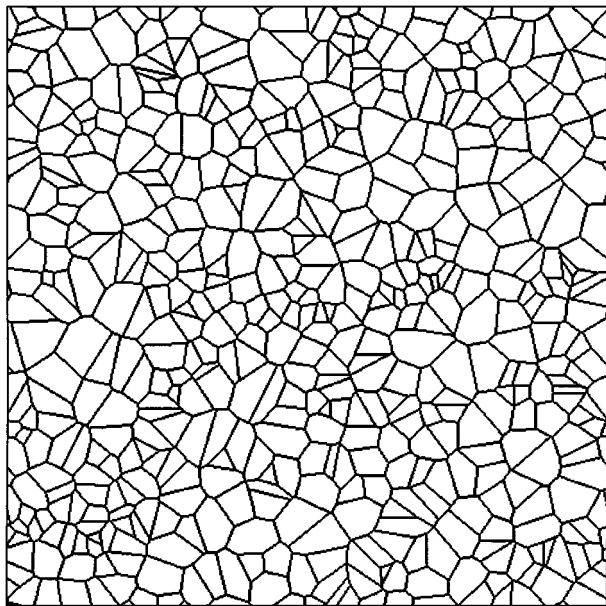
can be realized, particularly where fibres are suspended openly in etchant, which give rise to a variable angle, but always shallower with respect to the fibre axis. This leads to acute curved tips like rocket noses. But in all our observations, there appears to be this limiting angle, sometimes seen directly next to the original flat surface formed by cutting.

3.3. Mechanism of void formation

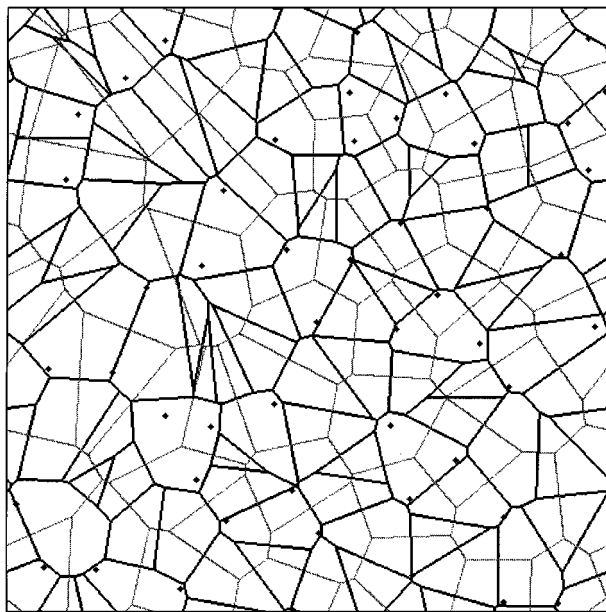
Although the conical craters at the top of each defect are features introduced by etching, their distribution relates directly to that of the defects themselves. It is evident in Fig. 2 that in all materials the craters appear in different sizes, which raises the question as to whether the size and arrangement of defects in these fibres is non-uniform, or non-random. This is very apparent in the Certran (a) with its larger average crater size, but it is also seen in the others. To answer these questions properly one would need, as is done later, to look in more detail at how such a distribution could arise. As well as the smaller crater size found in Spectra (b) and Tekmilon (d), there is in the Dyneema (c) a resistant skin to the fibre.

A proposed model for the development of the fibres themselves, and for the subsequent development of the observed etched morphology, is suggested by the manner in which fibres are formed. To remain entire, without failure, during the extension process the stress must be transmitted through the sample. This is believed to occur via the network of entangled molecules extending through the sample, which also manifests itself through shrinkage and thermal expansion behaviour [23], and chemocrystallization after cutting it with fuming nitric acid [17]. Such network components will suffer extension and so be rendered more efficient nucleating sites for further epitaxial growth, sharing the same chain axis orientation, into the spaces enclosed by the network. Fig. 4a shows how the first stage would apply to a random distribution of parallel nuclei. Remnants of such structures are seen on partial melting and recrystallization of fibres [24]. If all growth starts simultaneously these cylinders would impinge along linear boundaries, which if observable would give a "crazy-paving" pattern similar to the impingement pattern of spherulites in 2-dimensional growth in a thin film [25]. The volume deficit on crystallization would, in a rigid framework, produce a negative pressure leading possibly to voids, or to regions of increased free volume. This might also be a significant factor in reducing the supercooling of the last material to crystallize next to these regions, thereby coarsening their texture to the point where it is observable [26]. In polypropylene, which gives large spherulites, it is quite common to see large voids at the surface [27] of films, and it is possible to observe these in the interior of specimens by, for example, exciting a discharge in the attenuated air they contain with radio-frequency [28]. It is to be noted that a random distribution of nuclei gives the appearance of dense and sparse regions.

After sufficient etching the circular cones will merge to give linear boundaries in the manner of a Voronoi



(a)



(b)

Figure 4 (a) An impingement pattern generated by outward growth from randomly placed nuclei, (b) growth from a more uniform arrangement of nuclei; *thin line*: the impingement pattern generated by growth; *thick line*: a network of crater tops which would result from etching out of voids at the intersections of the impingement pattern.

network. The statistical properties of this process are such as to give an appearance of non-uniformity even when the nuclei are randomly distributed [29]. Indeed, the actual appearance is better simulated with a model containing a larger number of initial nuclei, then finding which pairs of nuclei were closest, and removing one, until 50% of the nuclei were removed Fig. 4b. The first stage of development gives the impingement pattern shown as fainter lines. The defects occur at the triple junctions. On subsequently etching the transverse section of the fibre the conical structures develop outwards from the voids. These also impinge to give a "crazy-paving" pattern, which is in a way, the inverse

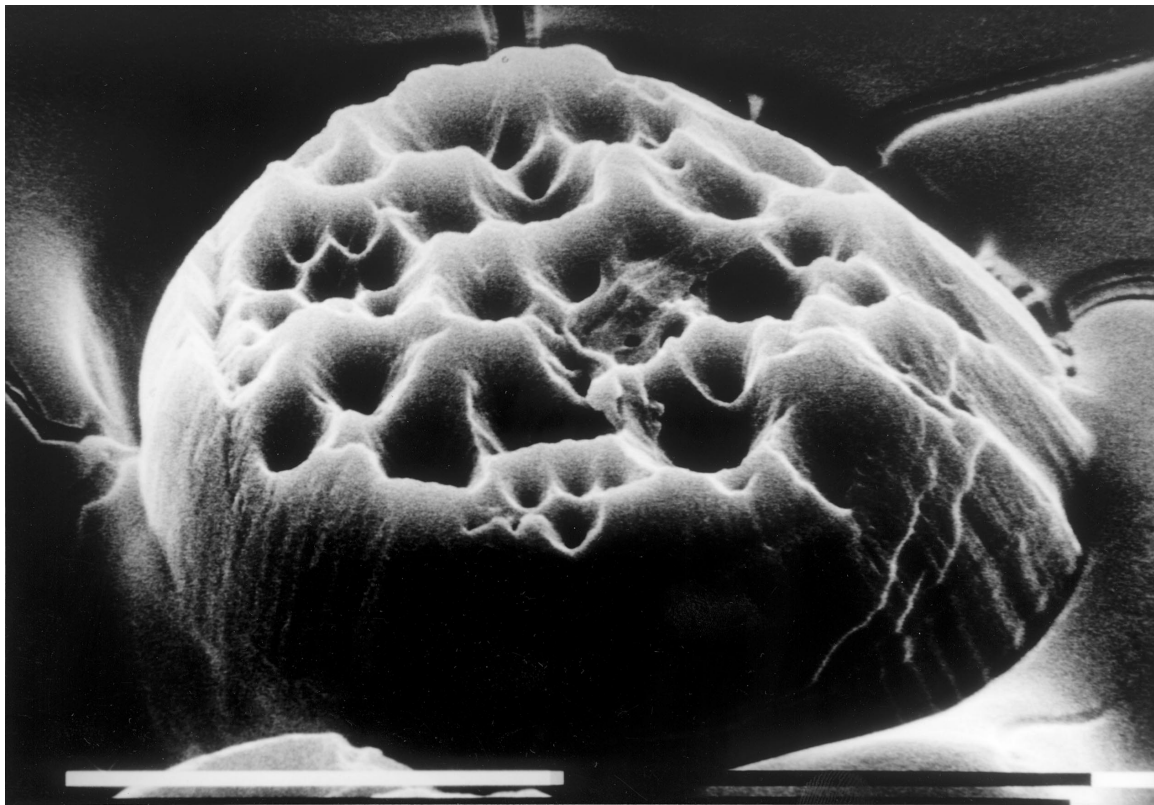
of the impingement pattern, shown in thick lines. The original pattern is not seen directly in the etched specimen, because of the very fine general texture of the material, and is only inferred from its effect in initiating the conical craters at the three-way impingement points.

By changing the composition of the etchant it is possible to alter the way in which this structure is presented. The dry etchant used for the specimens in Fig. 5 rather than the wetter etchant used for the previous two figures is inferred to be less able to penetrate the tiniest holes, and so the difference between the melt and solvent spun materials is not brought out so well. In the Certran (a) the attack down from the surface may have been inhibited in some regions (perhaps due to cutting damage), and so some circular profiles are observed where conical etch pits have not yet met their neighbours. In the case of the Spectra fibre (b), the drier etchant is opening up cones much faster in the more open defects relative to their smaller neighbours, and so certain large cones have obliterated their neighbours which might have transiently been present. In the Dyneema (c) there is in addition a prominent raised rim which derives from the skin-core structure of this material. The very narrow outside skin observed in Fig. 2c is now being attacked diagonally, probably making the resistant skin layer appear thicker than it initially is.

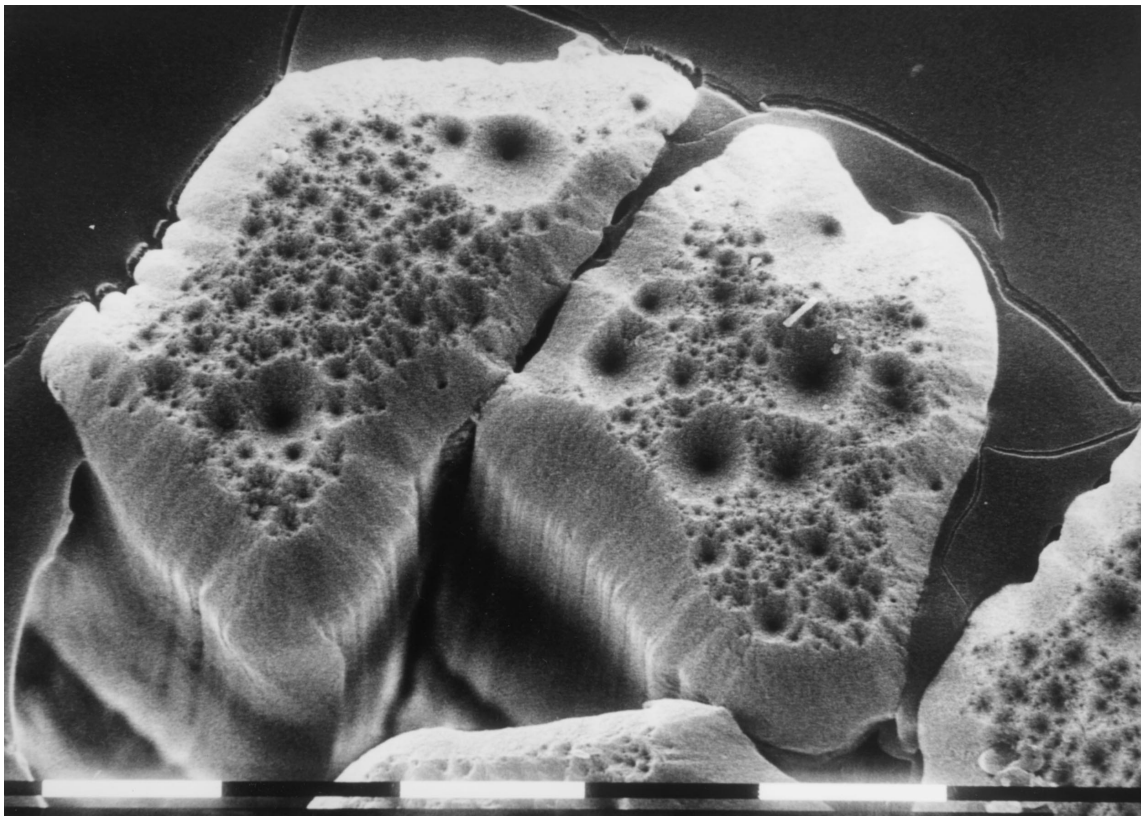
3.4. Longitudinal sections

These are seen in Fig. 6. *For the most part, well defined lamellar textures are absent, these fibre morphologies are thus of a different kind from those crystallized in the absence of stress.* The density deficient regions are not so easily displayed when the etchant approaches from the side, but certain features do appear, for example those shown for Certran (arrowed in Fig. 6a). They are seen much more prominently in the PE fibres processed with solvent, both the gel-spun fibres Spectra and Dyneema Fig. 6b and c and melt-kneaded Tekmilon 6d, since in these they are marked out by the presence of tiny recrystallized lamella-like entities in a shish-kebab type formation. These may have been generated as secondary growths in the density deficient regions during a final heating stage during the fibre manufacture. In Certran this lamellar decoration only appear after this material is heated in the compaction process [2]. For each material the lengths of these observed defects have been measured and averaged, giving the results in Table I. There appears to be a correlation of average length with the square root of the weight average MW, but it would require observation of different molecular weights treated by the same process, or of one material treated by variations of the same process, to judge how significant this is.

The melting of Certran fibres proceeds gradually over a few degrees, with differential melting starting from the density deficient regions, and proceeding sideways in a cylindrical fashion [3]. After cooling, where there was once a very thin void there now exists a cylindrical region filled with lamellae, which share the



(a)



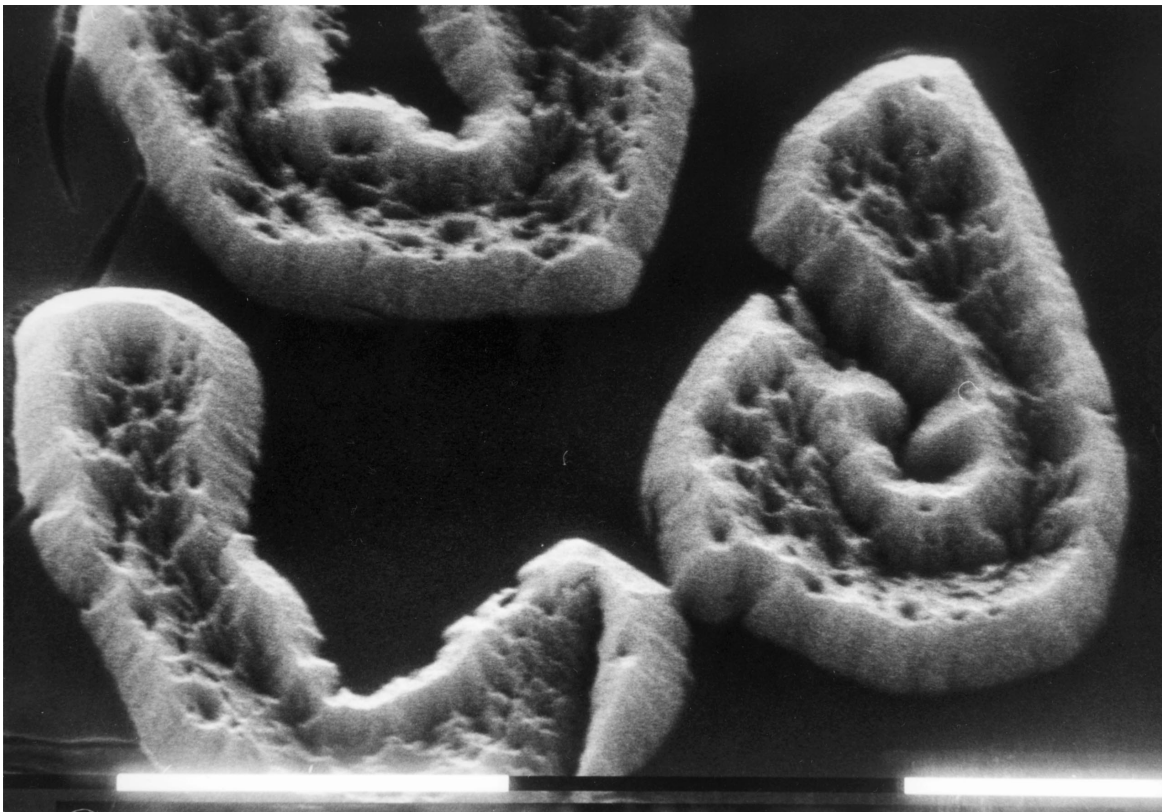
(b)

Figure 5 Morphology of fibre cross-sections etched with “dry” etch: (a) Certran, (b) Spectra, (c) Dyneema and (d) Tekmilon. SEM of specimens at lower magnification (a) tilted (b, c, d) untilted. All bars = 10 μm . (*Continued*)

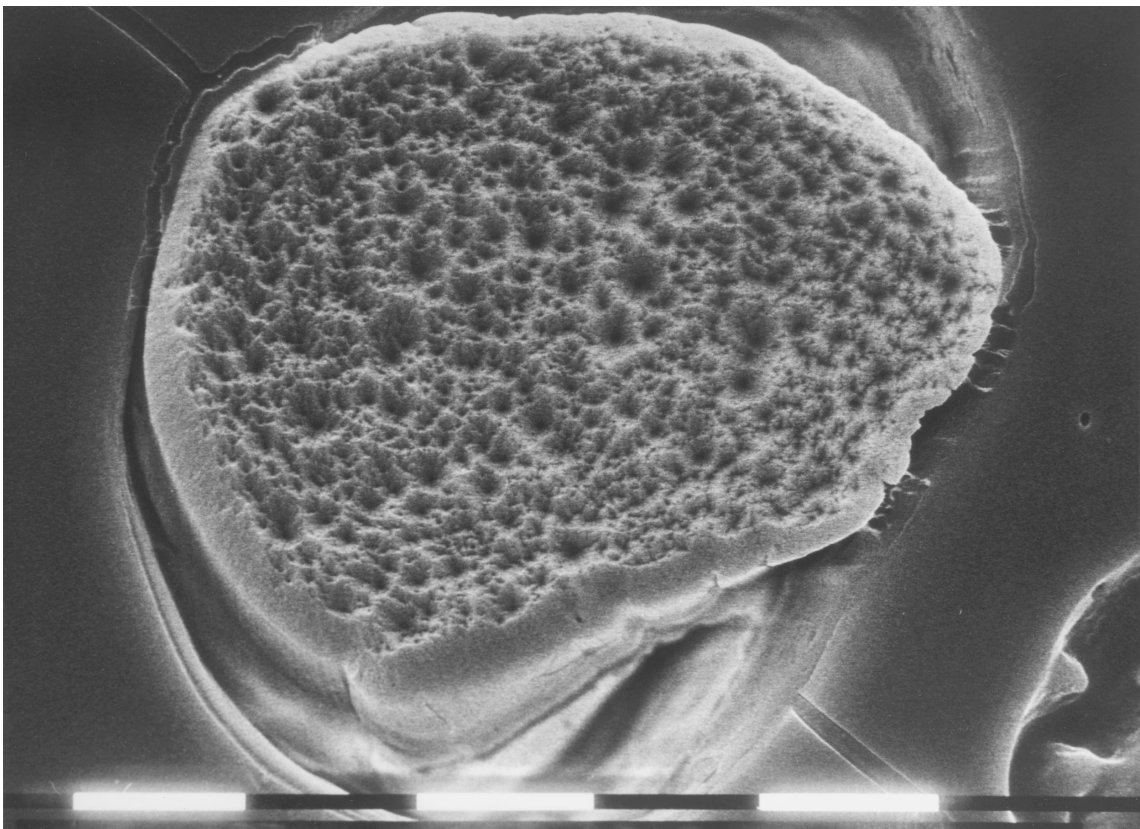
crystallographic orientation of the fibre, so that they are observed flat on with their basal surfaces in cross-section. As the previous work showed, the unmelted surround still etched with the diagonal profile, but the

lamellar basal surfaces are resistant to etching, giving a flat interior like a pool in a volcanic crater.

The gel-spun fibres melt over a much narrower range, particularly when held in compactions. In Spectra, most



(c)

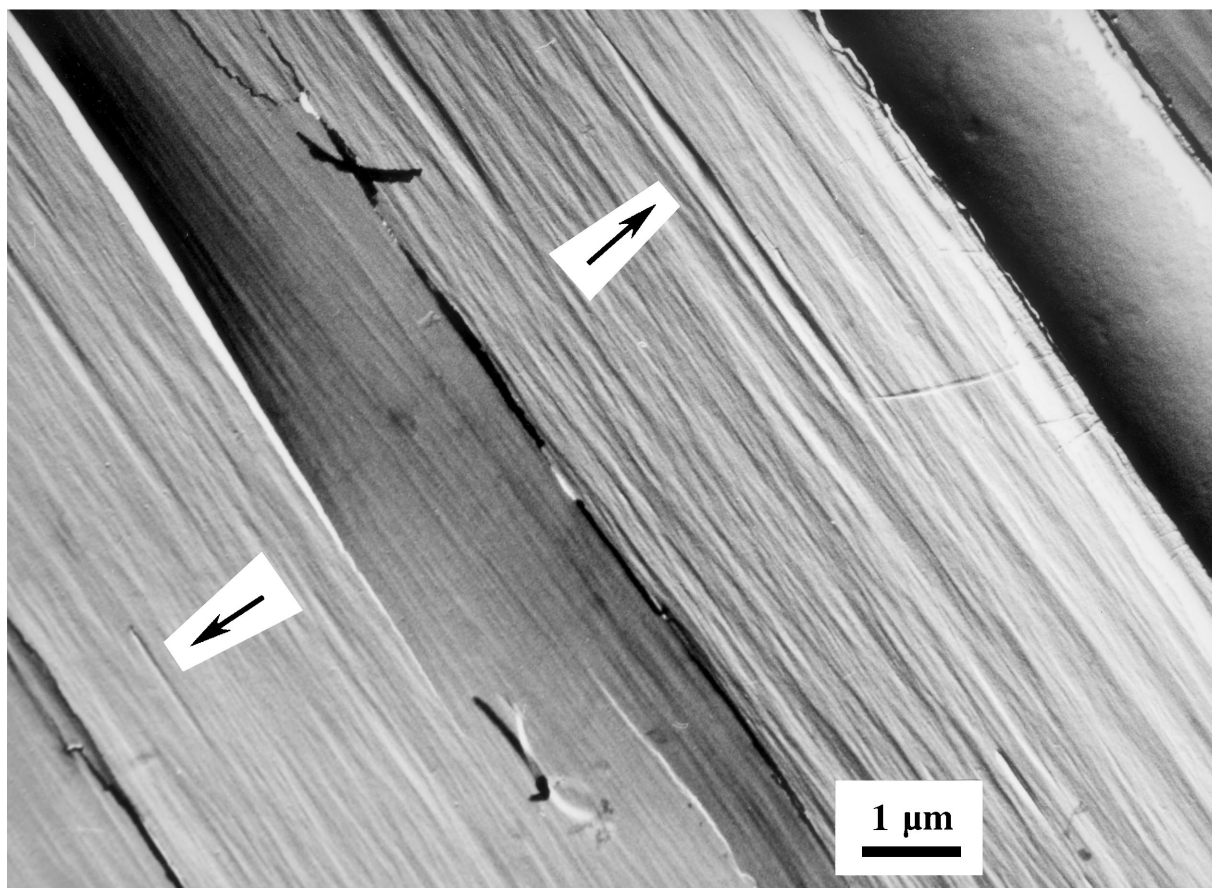


(d)

Figure 5 (Continued).

of the morphological change resulting from melting is observed between compactions carried out at 154 and 155 °C [21]. The partially melted morphology is different, since it appears that the entangled network survives

in the form of “spines”, which are somewhat ribbon-like row nuclei on which the molten majority of the fibre can recrystallize, and which are seen to be increasingly separated as treatment temperature increases [24].

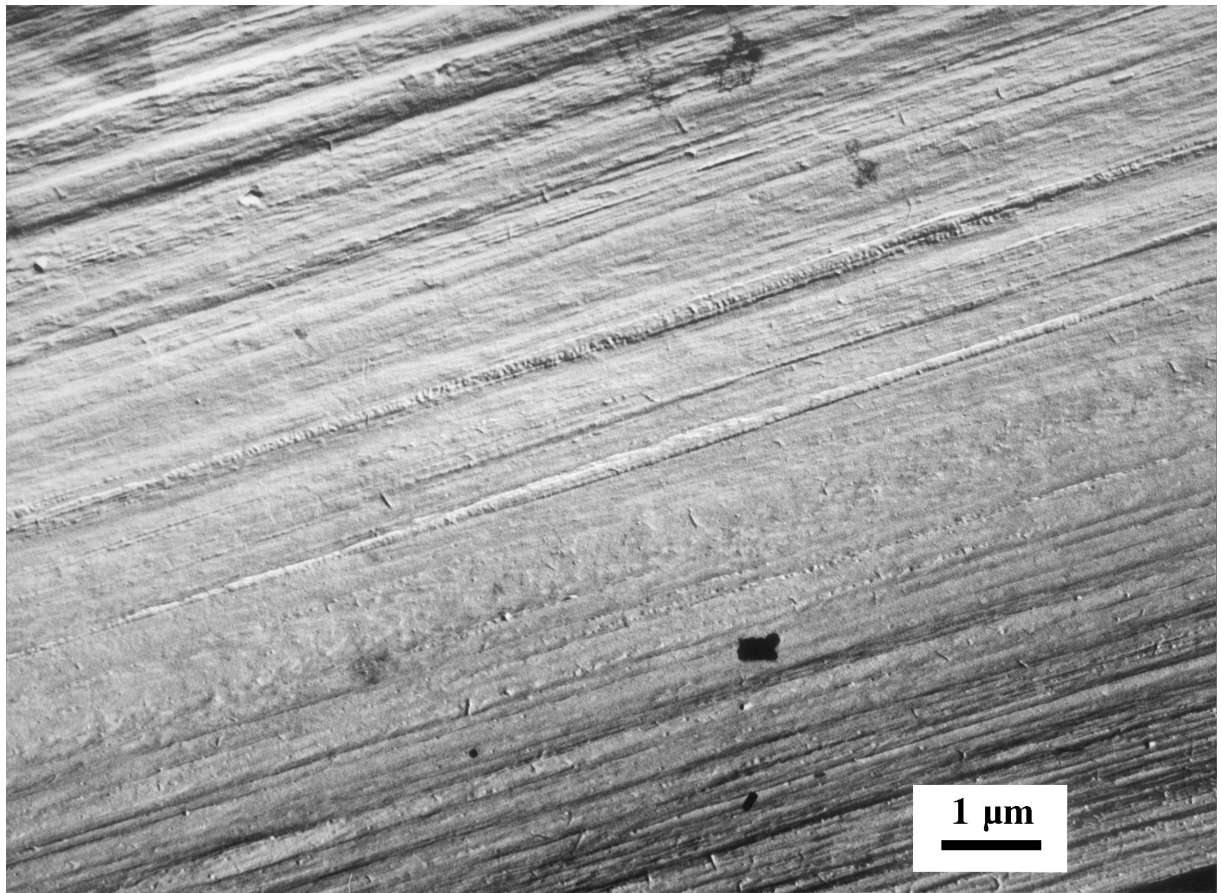


(a)

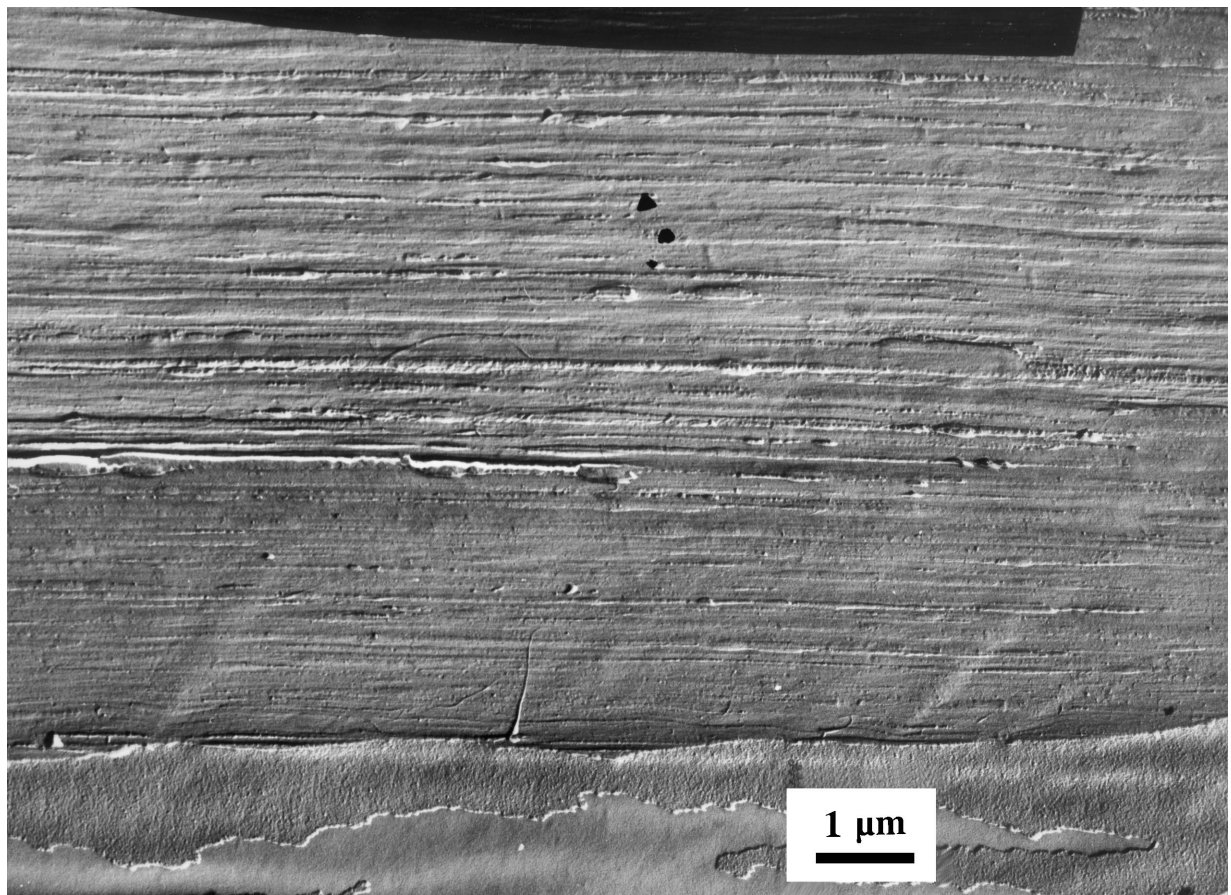


(b)

Figure 6 Morphology of fibre longitudinal sections etched with "long wet" etch: (a) Certran, (b) Spectra, (c) Dyneema and (d) Tekmilon. TEM of untilted specimens. (Continued)

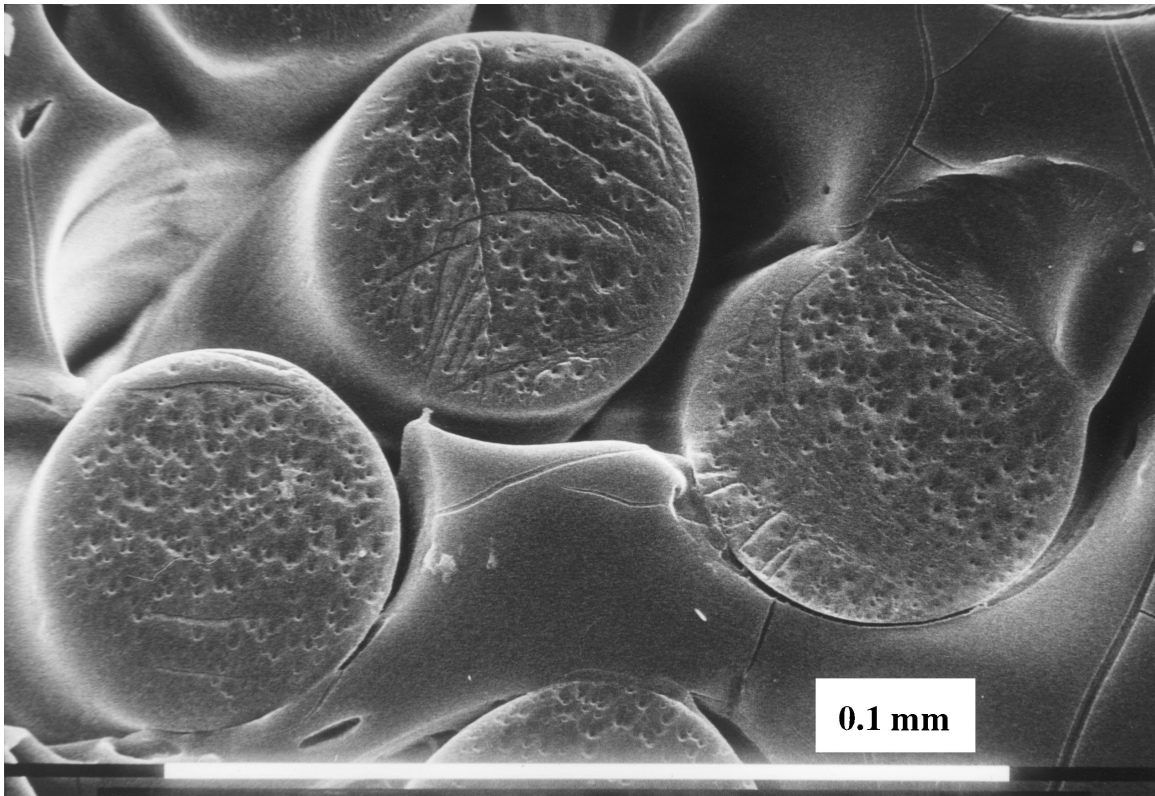


(c)

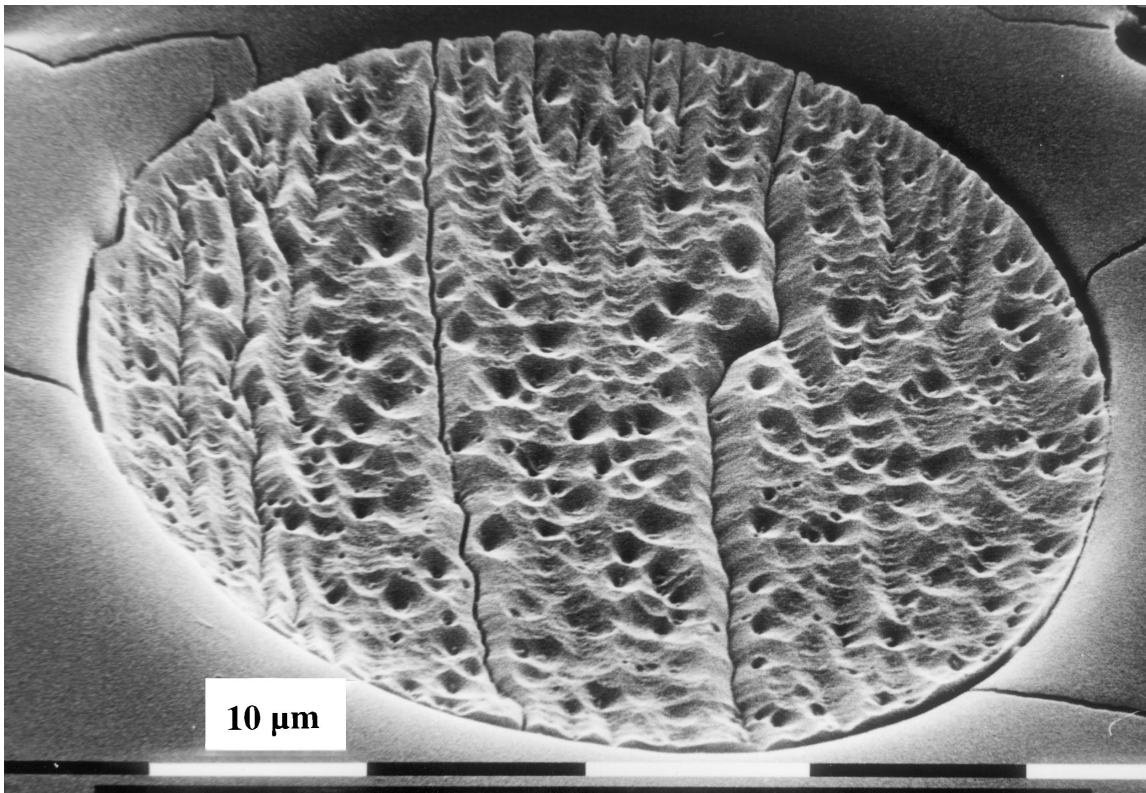


(d)

Figure 6 (Continued).



(a)



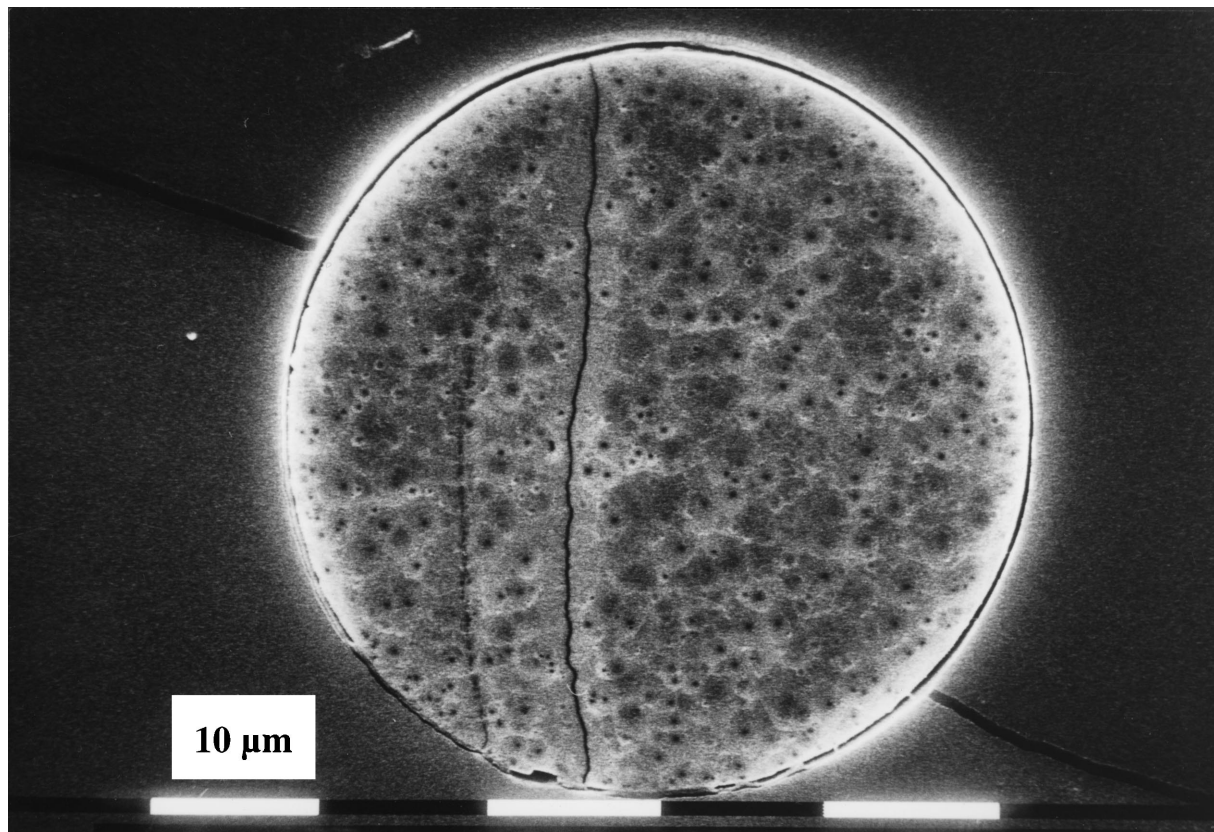
(b)

Figure 7 Polypropylene fibres, seen in transverse section: (a) untilted and (b) tilted after “short wet” etch and (c) untilted after “dry” etch; and (d) in longitudinal section after “long wet” etch. (Continued)

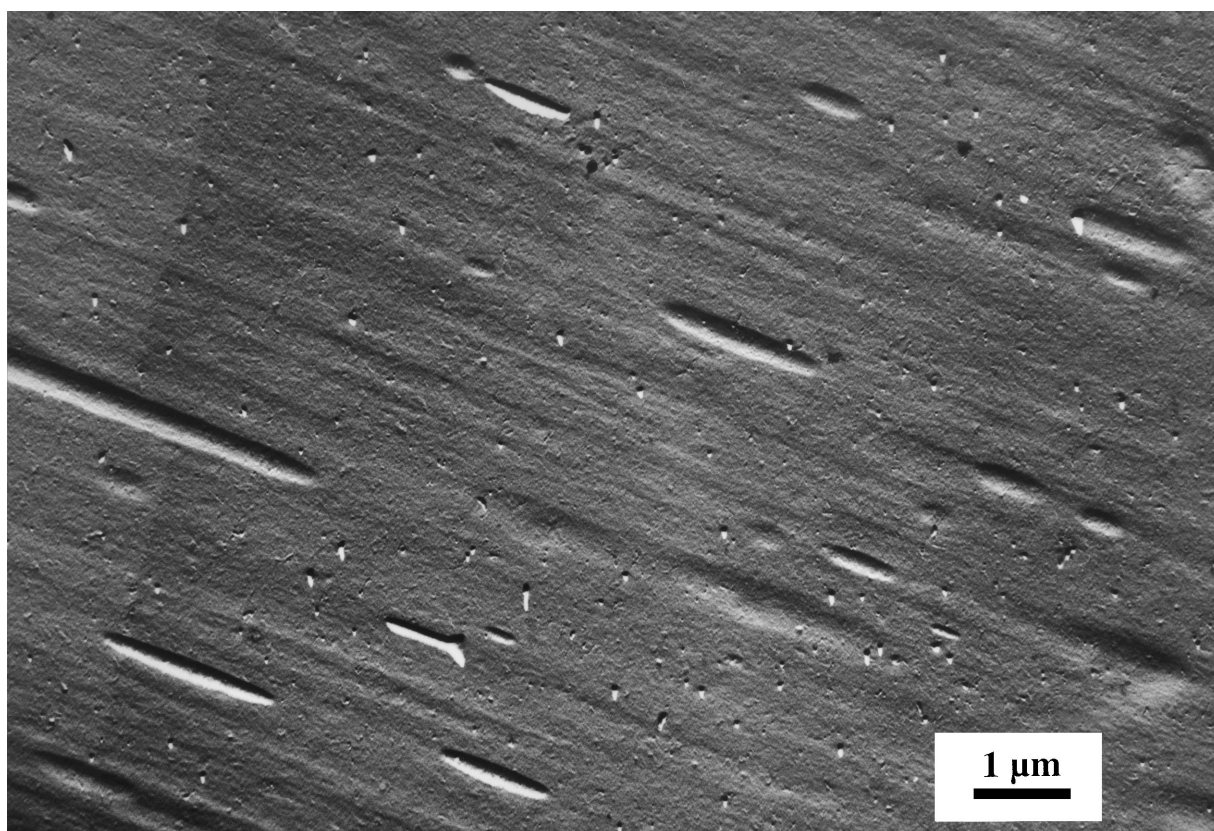
3.5. Polypropylene

In transverse section Fig. 7a the PP fibre is circular as would again be expected for a melt spun system. In another specimen Fig. 7b instead of circular void craters

there appear V-shaped trenches around crack-like defects. Fig. 7c shows several fibres with different concentrations of defects in different directions. These crack-like defects are not correlated with the cutting direction,



(c)



(d)

Figure 7 (Continued).

so it appears that they are a feature of the fibres, perhaps due to mechanical damage in the final phase of fibre production. Here, the voids do not always etch out into such an impinging network of conical craters as

seen in PE, but the conical craters often appear isolated among more shallow craters. This may be because the voids are in general much shorter and as seen in longitudinal section have much better defined ends Fig. 7d.

However, the general etching mechanism appears to be the same as in PE, even though the PP molecules are packed helically into the crystal.

4. Conclusions

1. A new model of fibre structure has been developed, based on etching of advanced PE and PP fibres with permanganic reagents. This reveals well defined substructures developed during the crystallization process.

2. Each of the four commercial PE fibres examined differs from the others in its characteristic outline and internal substructure.

3. It is proposed that the substructure is a consequence of nucleation on an extended network of entangled molecules permeating the fibres. Subsequent growth into spaces between the network will encounter stresses due to the contraction on crystallization leading to distributed density deficient regions of high free volume.

4. Free volume is available in the fibres, which will dictate the pattern of melting in applications such as productions of composites by high-temperature compaction.

Acknowledgements

The Authors thank Dr P.J. Hine of the IRC in Polymer Science and Technology, University of Leeds, for the supply of the fibres, and Dr P.A. Mulheran of the Physics Department, University of Reading, for the Voronoi network calculations.

References

1. P. J. HINE, I. M. WARD, R. H. OLLEY and D. C. BASSETT, *J. Mater. Sci.* **28** (1993) 316.
2. R. H. OLLEY, D. C. BASSETT, P. J. HINE and I. M. WARD, *ibid.* **28** (1993) 1107.
3. M. A. KABEEL, R. H. OLLEY, D. C. BASSETT, P. J. HINE and I. M. WARD, *ibid.* **29** (1994) 4694.
4. *Idem.*, *ibid.* **30** (1995) 601.

5. M. I. ABO EL MAATY, D. C. BASSETT, R. H. OLLEY, P. J. HINE and I. M. WARD, *ibid.* **31** (1996) 1157.
6. M. I. ABO EL MAATY, PhD thesis Mansoura, Egypt, 1995.
7. P. J. LEMSTRA, R. KIRSCHBAUM, T. OHTA. and H. YASUDA, in "Developments in Oriented Polymers-2 (Chapter 2)," edited by I. M. Ward (Elsevier Science Publishers, London, 1987).
8. J. J. POINT, M. GILLIOT, M. DOSIERE and A. GOFFIN, *J. Polym. Sci.* **C38** (1972) 261.
9. A. WAWKUSCHEWSKI, H. J. CANTOW, S. N. MAGONOV, J. D. HEWES and M. A. KOCUR, *Acta Polymerica* **46** (1995) 168.
10. J. P. PENNING, A. A. DE VRIES, J. VAN DER VEN and A. J. PENNING, *Phil. Mag. A* **69** (1994) 267.
11. J. A. ODELL, D. T. GRUBB and A. KELLER, *Polymer* **19** (1978) 617.
12. D. C. PREVORŠEK, in "The Handbook of Fiber Science and Technology, Vol.3, High Technology Fibers," edited by M. Lewin and J. Preston, pp. 1-170.
13. A. SCHAPER, D. ZENKE, E. SCHULTZ, R. HIRTE and M. TAEGER *Phys. Status. Solid.* **A116** (1989) 179.
14. D. C. BASSETT, in "Developments in Crystalline Polymers-2 (Chapter 2)," edited by D. C. Bassett (Applied Science Publishers, London, 1988).
15. G. CAPACCIO and I. M. WARD, *J. Polym. Sci., Polym. Phys. Ed.* **19** (1981) 667.
16. *Idem.*, *ibid.* **20** (1982) 1107.
17. N. KHOSRAVI, S. B. WARNER, N. S. MURTHY and S. KUMAR, *J. Appl. Polym. Sci.* **57** (1995) 781.
18. T. AMORNSAKCHAI, D. L. M. CANSFIELD, S. A. JAWAD, G. POLLARD and I. M. WARD, *J. Mater. Sci.* **28** (1993) 1689.
19. P. J. BARHAM and A. KELLER, *ibid.* **20** (1985) 2281.
20. J. SMOOK and A. J. PENNING, *J. Appl. Polym. Sci.* **27** (1982) 2209.
21. R. J. YAN, P. J. HINE, I. M. WARD, R. H. OLLEY and D. C. BASSETT, *J. Mater. Sci.* **32** (1997) 4821.
22. R. H. OLLEY, *Sci. Prog. Oxf.* **70** (1986) 17.
23. I. M. WARD and P. J. HINE, *Polym. Eng. Sci.* **37** (1997) 1809.
24. J. TECKOE and M. I. ABO EL-MAATY in preparation.
25. A. GALESKI and E. PIORKOWSKA, *Coll. Polym. Sci.* **261** (1983) 1.
26. L. S. DONG, D. C. BASSETT and R. H. OLLEY, *J. Macromol. Sci. -Phys.* **B37** (1998) 527.
27. R. H. OLLEY and D. C. BASSETT, *ibid.* **B33** (1994) 209.
28. A. GALESKI and E. PIORKOWSKA, *J. Polym. Sci. -Phys. Ed.* **21** (1983) 1313.
29. P. A. MULHERAN, *Phil. Mag. Lett.* **66** (1992) 219.

Received 27 October

and accepted 18 November 1998